Electronic Supplementary Material (ESI) for Dalton Transactions

Supplementary information

Self-assembly of $[Cu^{II}Tb^{III}]^{3+}$ and $[W(CN)_8]^{3-}$ tectons: a case study of a mixture containing two complexes showing slow-relaxation of the magnetization

Diana Visinescu, Ie-Rang Jeon, Augustin M. Madalan, Maria-Gabriela Alexandru,
Bogdan Jurca,Corine Mathonière,Rodolphe Clérac and Marius Andruh

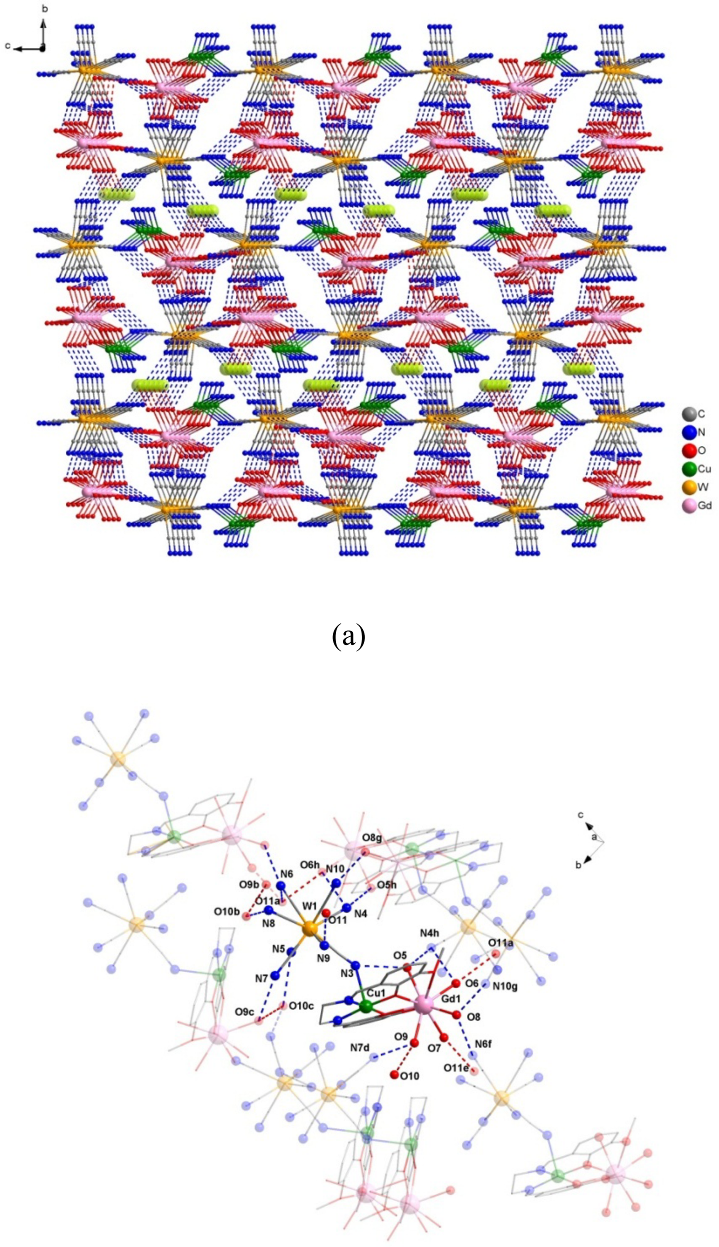

Fig. S1. Perspective view of: (a) a fragment of three-dimensional hydrogen-bond network (the water crystallization molecules, are represented as space-filling); (b) details of packing highlighting N···O (blue dotted line) and O···O (red dotted lines) type bonds (symmetry codes: *a* = 1-*x*, -*y*, 2-*z*; *b* = *x*, *y*, 1+*z*, *c* = 0.5+*x*, 0.5-*y*, 0.5+*z*; *d* = -0.5+*x*, 0.5-*y*, -0.5+*z*; *e* = *x*, *y*, -1+*z*; *f* = -1+*x*, *y*, -1+*z*; *g* = 1-*x*, -*y*, 2-*z*; *h* = 2-*x*, -*y*, 2-*z*) in compound **1.**

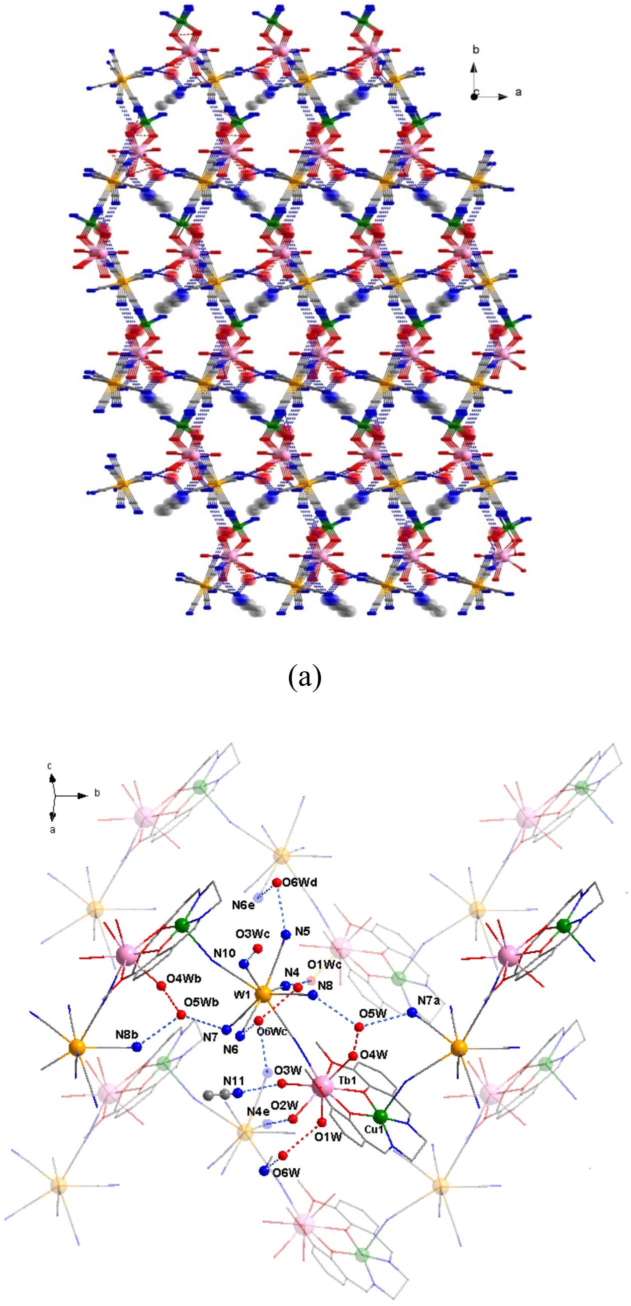

(a)

(b)

Fig. S2. Perspective view of: (a) a fragment of three-dimensional hydrogen-bond network (the crystallization molecules, water and acetonitrile are represented as space-filling); (b) details of packing highlighting N···O (blue dotted line) and O···O (red dotted lines) type bonds (symmetry codes: *a* = 1-*x*, 0.5+*y*, 1-*z*; *b* = 1-*x*, -0.5+*y*, 1-*z*; *c* = *x*, *y*, 1+*z*; *d* = -1+*x*, *y*, 1+*z*; *e* = -1+*x*, *y*, *z*) in compound **2.**

Both compounds, **1** and **2**, bear water molecules and terminal cyanide ligands able to establish hydrogen-bonds: O···O and O···N type (the intra- and intermolecular H-bonds distances are gathered in table S2). The crystal packing for the two complexes reveal the formation of the three-dimensional supramolecular networks, in which the lattice/coordinated H_2O molecules and free cyanide groups intra- and inter-connect the trinuclears complexes/chains (fig. S1 and S2).

Table S1. Selected bond lengths [Å], angles [^{O}] and contact distances [Å] for **1** and **2**

1	**2**
Cu1-O2 = 1.923(4)	Cu1-O2 = 1.910(4)
Cu1-O3 = 1.901(4)	Cu1-O3 = 1.908(4)
Cu1-N1 = 1.906(5)	Cu1-N1 = 1.914(5)
Cu1-N2 = 1.920(6)	Cu1-N2 = 1.937(5)
Tb1-O1 = 2.671(5)	Tb1-N3 = 2.481(4)
Tb1-O2 = 2.336(4)	Tb1-O1 = 2.585(3)
Tb1-O3 = 2.323(4)	Tb1-O2 = 2.361(4)
Tb1-O4 = 2.676(4)	Tb1-O3 = 2.317(4)
Tb1-O5 = 2.406(4)	Tb1-O4 = 2.317(4)
Tb1-O6 = 2.404(4)	Tb1-O1W = 2.407(4)
Tb1-O7 = 2.421(5)	Tb1-O2W = 2.447(4)
Tb1-O8 = 2.396(5)	Tb1-O3W = 2.425(4)
Tb1-O9 = 2.461(4)	Tb1-O4W = 2.406(4)
W1-C19 = 2.160(6)	W1-C19 = 2.157(5)
W1-C20 = 2.161(6)	W1-C20 = 2.162(5)
W1-C21 = 2.158(6)	W1-C21 = 2.167(6)
W1-C22 = 2.160(6)	W1-C22 = 2.152(6)
W1-C23 = 2.152(6)	W1-C23 = 2.166(6)
W1-C24 = 2.157(6)	W1-C24 = 2.156(5)
W1-C25 = 2.157(6)	W1-C25 = 2.164(5)
W1-C26 = 2.156(5)	W1-C26 = 2.156(5)
Cu1-N3-C19 = 131.339(560)	Cu1-N9-C25 = 148.061(500)
W1-C19-N3 = 174.836(595)	W1-C25-N9 = 177.998(541)
Cu1-O2-Tb1 = 104.08(18)	Cu1-O2-Tb1 = 104.00(15)
Cu1-O3-Tb1 = 105.33(18)	Cu1-O3-Tb1 = 105.74(15)
	W1-C19-N3 = 176.277(479)
	Tb1-N3-C19 = 172.957(444)
Cu1-Tb1 = 3.3676(7)	Cu1-Tb1 = 3.3776(7)
	W1-Tb1 = 5.7787(3)

Table S2. The length values for H-bonds for **1** and **2**(Å)

1		**2**	
O9···O10	2.7276(1)	O1W···O6W	2.6661(8)
O7···O11^{e}	2.7547(8) Å	O4W···O5W	2.7349(8)
O6···O11^{a}	2.8139(1) Å	O2W···N4^{e}	2.8874(8)
N3···O5	2.9616(9) Å	O3W···N11	2.8566(1)
N4···O5^{h}	2.8111(9) Å	O5W···N7^{a}	2.9507(1)
N5···O10^{c}	3.0735(1) Å	O5W···N8	2.9220(9)
N6···O11^{a}	3.0555(1) Å	N5···O6W^{d}	2.7881(1)
N7···O9^{c}	2.8594(1) Å	N6···O6W^{c}	2.9943(1)
N8···O10^{b}	2.8919(1) Å	N10···O3W^{c}	2.7172(9)
N10···O8^{g}	2.8509(1) Å		

Symmetry codes: *a* = 1-*x*, -*y*, 2-*z*; *b* = *x*, *y*, 1+*z*, *c* = 0.5+*x*, 0.5-*y*, 0.5+*z*;*e* = *x*, *y*, -1+*z*;*g* = 1-*x*, -*y*, 2-*z*; *h* = 2-*x*, -*y*, 2-*z* (**1**); *a* = 1-*x*, 0.5+*y*, 1-*z*; *c* = *x*, *y*, 1+*z*; *d* = -1+*x*, *y*, 1+*z*; *e* = -*1*+*x*, *y*, *z* (**2**)

IR spectroscopy data for compounds **1** and **2**:

IR (KBr, cm^{-1}):

(**1**) 3530(w), 3335(m), 2975(w), 2840(w), $\bar{\nu}$ **(C≡N):** 2164(w), 2151(m), 2144(w), 2135(w), $\bar{\nu}$ **(C=N):** 1633(s), 1466(m), 1388(w), 1280(m), 1222(m), 1074(w), 960(w), 740(m);

(**2**) 3525(w), 3330(m), 2980(w), 2843(w), $\bar{\nu}$ **(C≡N):** 2182(m), 2162(w), 2153(w), 2140(w), $\bar{\nu}$ **(C=N):** 1630(s), 1464(m), 1390(w), 1275(m), 1222(m), 1070(w), 950(w), 745(m)

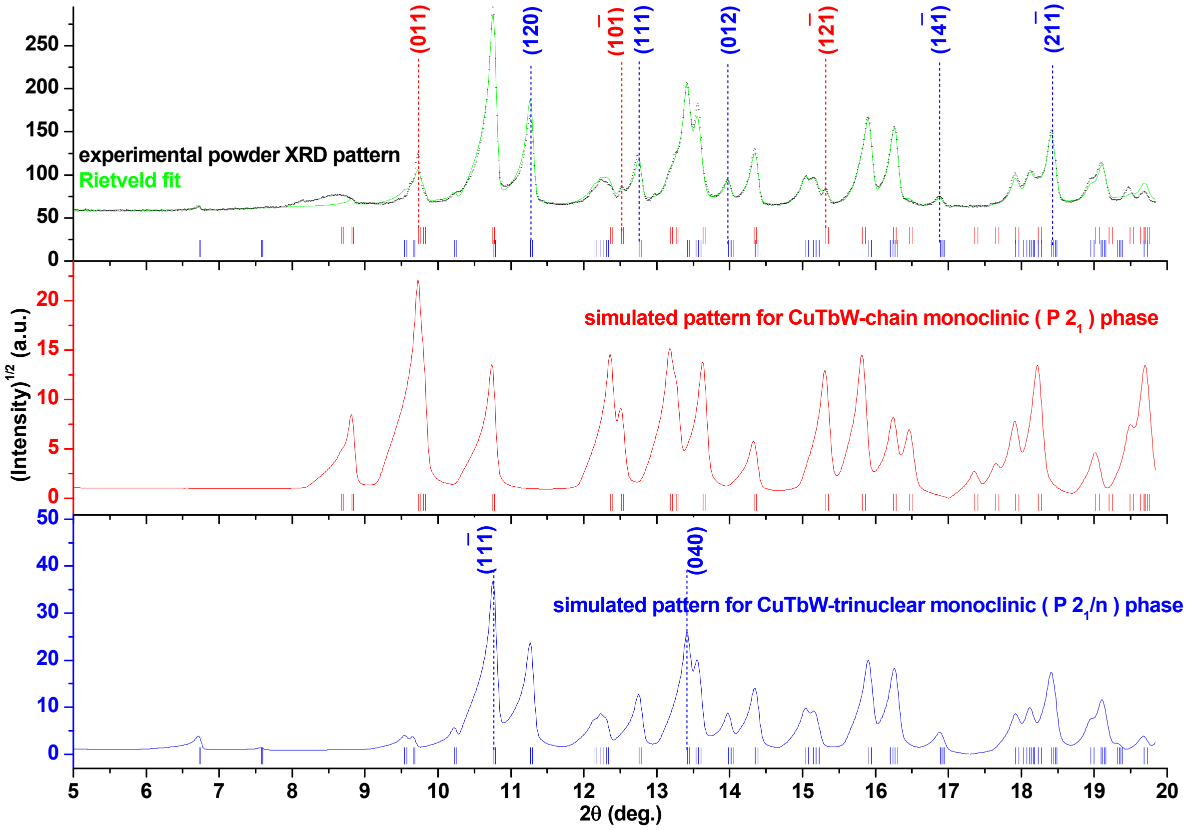

Fig. S3. Experimental, fitted and simulated powder XRD patterns for the mixture of **1** and **2** samples and for each phase. The positions of Bragg reflections are marked with short vertical lines. The indexing of the distinctive diffraction peaks is presented for each phase on the experimental XRD pattern.

Experimental

Room temperature X-ray powder diffraction data were acquired on a Shimadzu XRD-7000 diffractometer (Bragg-Brentano geometry) using CuKα radiation, operated at 40 kV and 30 mA in the 2θ range 5-20° with steps of 0.01° and a counting time of 60 s/step. The rotational speed of the sample was set to π/2 rad·s^{-1}.

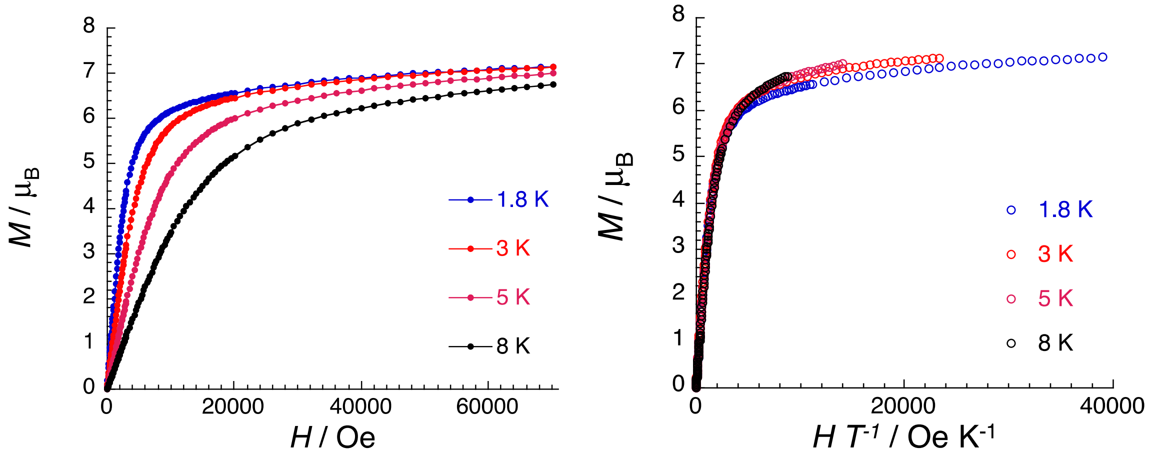

Fig. S4. Plots of *M vs*. *H* (left) and *Mvs*. *H/T* (right) at different temperatures for sample B(or **1**).

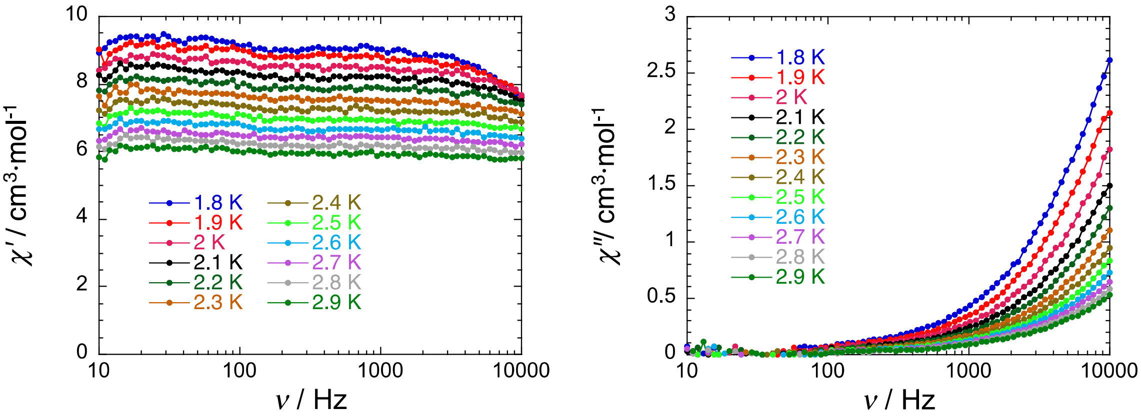

Fig. S5. Plots of χ' (left) and χ'' (right) *vs.* ν measured on the temperature range: 1.8-2.9 K for sample B(or **1**) in zero-dc field.

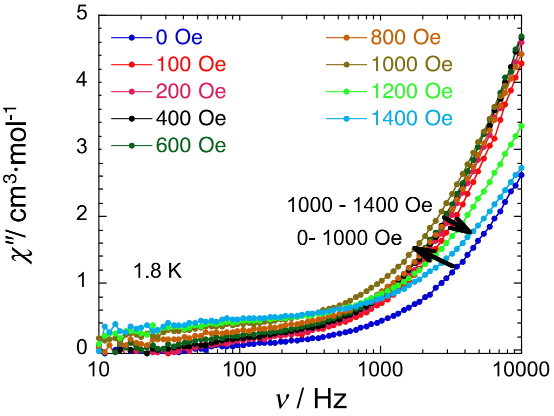

Fig. S6. *χ''vs. ν* plot measured at 1.8 K in dc fields ranging from 0-1000 Oe and 1000-1400 Oefor sample B(or **1**).